Inorganic Chemistry

ARTICLE

pubs.acs.org/IC

Homochiral Nickel Coordination Polymers Based on Salen(Ni) Metalloligands: Synthesis, Structure, and Catalytic Alkene Epoxidation

Yuanbiao Huang, Tianfu Liu, Jingxiang Lin, Jian Lü, Zujin Lin, and Rong Cao*

State Key Laboratory of Structural Chemistry, Fujian Institute of Research on the Structure of Matter, Chinese Academy of Science, Fuzhou 350002, China

Supporting Information

ABSTRACT: One-dimensional (1D) homochiral nickel coordination polymers $[Ni_3(bpdc)(RR\text{-}L)_2\cdot(DMF)]_n$ (**2R**, *RR*-L = (*R*,*R*)-(-)-1,2-cyclohexanediamino-*N*,*N*′-bis(3-*tert*-butyl-5-(4-pyridyl)salicylidene), bpdc = 4,4′-biphenyldicarboxylic acid) and $[Ni_3(bpdc)(SS\text{-}L)_2\cdot(DMF)]_n$ (**2S**, *SS*-L = (*S*,*S*)-(-)-1,2-cyclohexanediamino-*N*,*N*′-bis(3-*tert*-butyl-5-(4-pyridyl)salicylidene) based on enantiopure pyridyl-functionalized salen(Ni) metalloligand units NiL ((1,2-cyclohexanediamino-*N*,*N*′-bis(3-*tert*-butyl-5-(4-pyridyl)salicylidene))Ni^{II}) have been synthesized and characterized by microanalysis, IR spectroscopy, solid-state UV−vis spectroscopy, thermogravimetric analysis (TGA), circular dichroism (CD) spectroscopy, cyclic voltammetric measurement, and powder and single crystal X-ray diffraction. Each NiL as unbridging pendant metalloligand uses one terminal pyridyl group to coordinate achiral unit (nickel and $bpdc^{2-}$) building a helical chain, while the other pyridyl group remains uncoordinated. Both **2R** and **2S** contain left- and right-handed helical chains made of the achiral building blocks, while the NiL as remote external chiral source is perpendicular to the backbone of the helices. The nickel coordination polymers **2R** and **2S** containing unsaturated active nickel center in metalloligand NiL can be used as self-supported heterogeneous catalysts. They show catalytic activity comparable with their homogeneous counterpart in alkene epoxidation and exhibit great potential as recyclable catalysts.

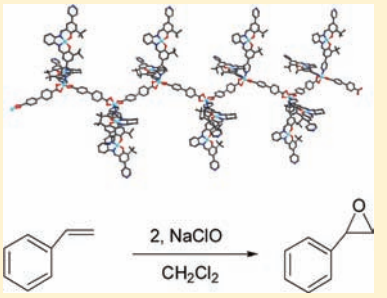

INTRODUCTION

Over the past decade, the use of transition metal complexes as catalysts for the olefin epoxidation has attracted considerable attention in academic and industrial fields.[1] Most of the publications concerned the use of highly enantioselective catalysts of (salen)Mn complexes developed by Jacobsen and Katsuki in the epoxidation of alkenes.[1−3] (Salen)Ni complexes, which have been used in homogeneous catalytic transformations such as the tetralin oxidation,[4] asymmetric aldol reaction,[5] Mannich-Type and Michael reactions,[6] also showed to be highly active for alkene epoxidation.[7−11] Although homogeneous catalysts usually exhibit high activity and selectivity in most of organic reactions, their practical applications remain limited because of catalyst instability and difficulty in catalyst/product separation. Immobilization of homogeneous catalysts can facilitate its recovery and reuse and therefore is of considerable interest to academia and industry.[12] Recently, a number of approaches have been developed for this purpose, typically including using inert inorganic materials or organic polymers as supports or conducting the reactions in some unconventional media such as ionic liquids or supercritical CO_2 fluid.[12,13] Although extremely successful, classical immobilization with various prefabricated supports is often plagued by negative effects such as reduction of catalytic activity and/or selectivity as a result of the poor accessibility, random anchoring, or disturbed geometry of the active sites in the solid matrix.[12,13] The immobilization of (salen)Ni complexes in heterogeneous catalysis has not been extensively explored. Some examples include the use of (salen)Ni complex immobilization in zeolites X and Y, as heterogeneous catalysts for the oxidation of phenol by H_2O_2[14] and for the epoxidation of cyclohexene[15] and *trans*-β-methylstyrene[10] by NaOCl. Corma used chiral (salen)Ni complexes immobilizing in ordered mesoporous silica supports (MCM-41), delaminated ITQ-2 and ITQ-6 zeolites, and amorphous silica for hydrogenation of imines.[16] Very recently, a sulfonato-salen-nickel(II) complex has been immobilized on a Zn(II)−Al(III) layered double hydroxide (LDH) host for tetralin oxidation.[4]

Infinite coordination polymers, especially metal−organic frameworks (MOFs) with infinite network structures built from organic bridging ligands and inorganic connecting nodes have been emerging as very promising materials for gas storage, separation, heterogeneous catalysis, sensing, and drug delivery.[17−33] Two different approaches have been utilized to synthesize catalytically active coordination polymers. The first method is the metal-connecting points with unsaturated coordination environments being utilized as catalytically active sites.[12,24−30] In the second one, catalytic sites are incorporated directly into the bridging ligands used to construct coordination polymers.[12,24−28,31−33] Although more synthetically demanding, the second approach is much more versatile and allows for the incorporation of a wide variety of catalysts, especially asymmetry catalysts.[25] Until now, a few

Received: August 31, 2010
Published: February 18, 2011

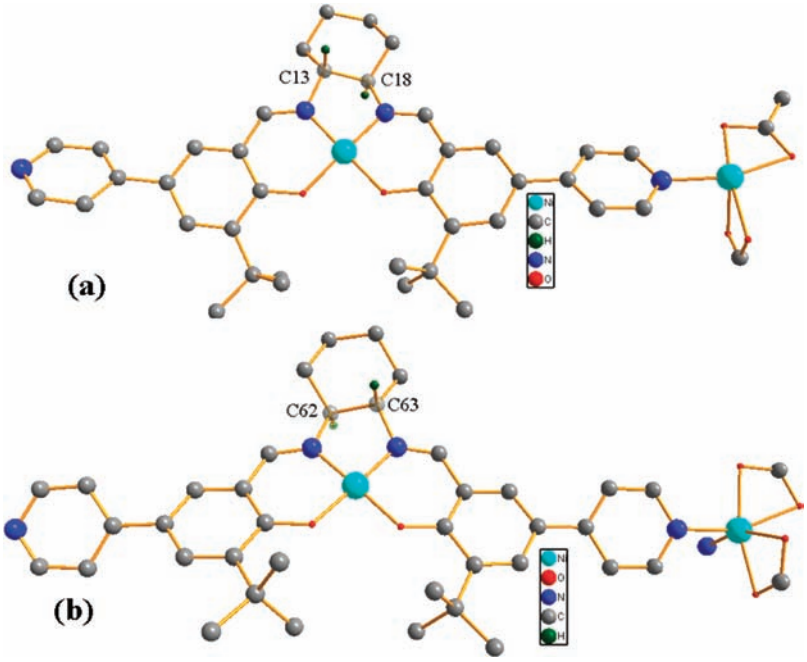

Figure 1. Perspective view showing the chirality of cyclohexyl groups in **2R** (a) and **2S** (b) (one of the two repeating units). Ligands bpdc, solvent molecules, and hydrogen atoms are omitted for clarity.

coordination polymers based on salen ligands with an additional functional group such as carboxylates,[34−42] *p*-benzoic acid groups,[43] and *p*-pyridyl groups[32,44,45] in the *para* or *meta* position to the OH group have been reported. There were only dipyridyl[32] and dicarboxylate[43b] functionalized (salen)MnCl metalloligands incorporating into the framework of structures of Zn-MOFs, and coordination polymers[33] formed by the reaction of [bis(catechol)-salen]Mn^{III} with several di- and trivalent metal ions using for highly effective olefin epoxidation. Herein, we report chiral dipyridyl functionalized nickel salen complexes NiL (**1R** and **1S**) as unbridging pendant metalloligands incorporating into infinite nickel coordination polymers as self-supported catalysts for alkene epoxidation.

RESULTS AND DISCUSSION

In a typical synthesis, the reaction of $Ni(OAc)_2 \cdot 4H_2O$ and chiral ligand (*R*,*R* or *S*,*S*)-(-)-1,2-cyclohexanediamino-*N*,*N*′-bis(3-*tert*-butyl-5-(4-pyridyl)salicylidene) (*RR*- or *SS*-)H_2L)[46] (1:1) in a MeOH solution at 60 °C resulted in yellow solids of *RR*-NiL (**1R**) and the enantiomer *SS*-NiL (**1S**). The orange crystals of **1S** suitable for single crystal X-ray diffraction were grown from the mixture of the solvent DMF/CH_2Cl_2/MeOH (1:1:1). The Ni^{II} ion is coordinated in nearly square-plane geometry with two nitrogen atoms and two oxygen atoms from the chelating L ligand (Supporting Information, Figure S1). The pyridyl groups of the L ligand are not involved in the coordination to the Ni^{II} ion, which can be used as metalloligands to assemble coordination polymers.

The chiral metalloligand **1R** or the enantiomer **1S** reacts with $Ni(NO_3)_2 \cdot 6H_2O$ and 4,4′-biphenyldicarboxylic acid (bpdc) (1:1:1) in a mixture of DMF and EtOH (10:1) at 80 °C after 24 h afforded the red brown needle crystals of **2R** or **2S** with high yields. The products **2R** and **2S** as nickel coordination polymers are stable in air and insoluble in water and common organic solvents formulated as $[Ni_3(bpdc)L_2 \cdot DMF]_n$ on the basis of single crystal X-ray diffraction, elemental analysis, and thermogravimetric analysis (TGA). Interestingly, **2R** and **2S** can also be prepared directly using chiral ligand (*RR*- or *SS*-)H_2L, $Ni(NO_3)_2 \cdot 6H_2O$, and bpdc (2:1:1) under the same conditions with high yields.

Single crystal X-ray diffraction study shows that both compounds **2R** and **2S** crystallize in the orthorhombic chiral space group $P222_1$ with absolute structure parameters of 0.028(1) and 0.055(2), respectively. X-ray crystallography shows that **2R** and **2S** are one-dimensional (1D) coordination polymers which have the same formula and are therefore isomorphous (Figure 1 and Supporting Information, Figure S1). Circular Dichroism (CD) spectra (Figure 4) of bulk materials **2R** and **2S** made from (*R*, *R*) and (*S*, *S*) enantiomers of the H_2L ligand are mirror images of each other, which indicates their enantiomeric nature.[41] The structures of the **2R** and **2S** are identical with the exception of being opposite hands of each other (Figure 1), and only that of **2R** is discussed here. There exist two different coordination models of the nickel(II) centers in **2R** (Figure 2). The coordination model of Ni2 is similar to that of Ni1, while Ni3 and Ni4 are similar to each other. One unsaturated nickel center Ni1 (Ni2) as active catalytic site from metalloligand NiL adopts nearly square geometry ($Ni-O_{avg}$ = 1.851 Å, $Ni-N_{avg}$ = 1.849 Å, Supporting Information, Table S1). The other nickel center ion Ni3 (Ni4) as metal node exhibits distorted octahedral coordination geometry, which is bridged by four oxygen atoms of the two different chelating $bpdc^{2-}$ ($Ni-O_{avg}$ = 2.121 Å) and two nitrogen atoms of the pyridyl groups from two different *cis*-NiL metalloligands ($Ni-N_{avg}$ = 2.051 Å). The coordination geometry around the metal node Ni3 (Ni4) is similar to that observed for the model complex dibenzoatodipyridinnenickel(II)[47a] (**5**) and polycatenated array of 1D nanotubes $[Ni_2(oba)_2(bpy)_2(H_2O)_2] \cdot bpy$ (**6**), which was obtained from the reaction of the rigid 4,4′-bipyridine (bpy) and the long V-shaped 4,4′-oxybis-(benzoate) (oba) ligands.[47b] However, interestingly, each metalloligand unit *RR*-NiL uses only one terminal pyridyl group to coordinate to a

dx.doi.org/10.1021/ic102181h |*Inorg. Chem.* 2011, 50, 2191–2198

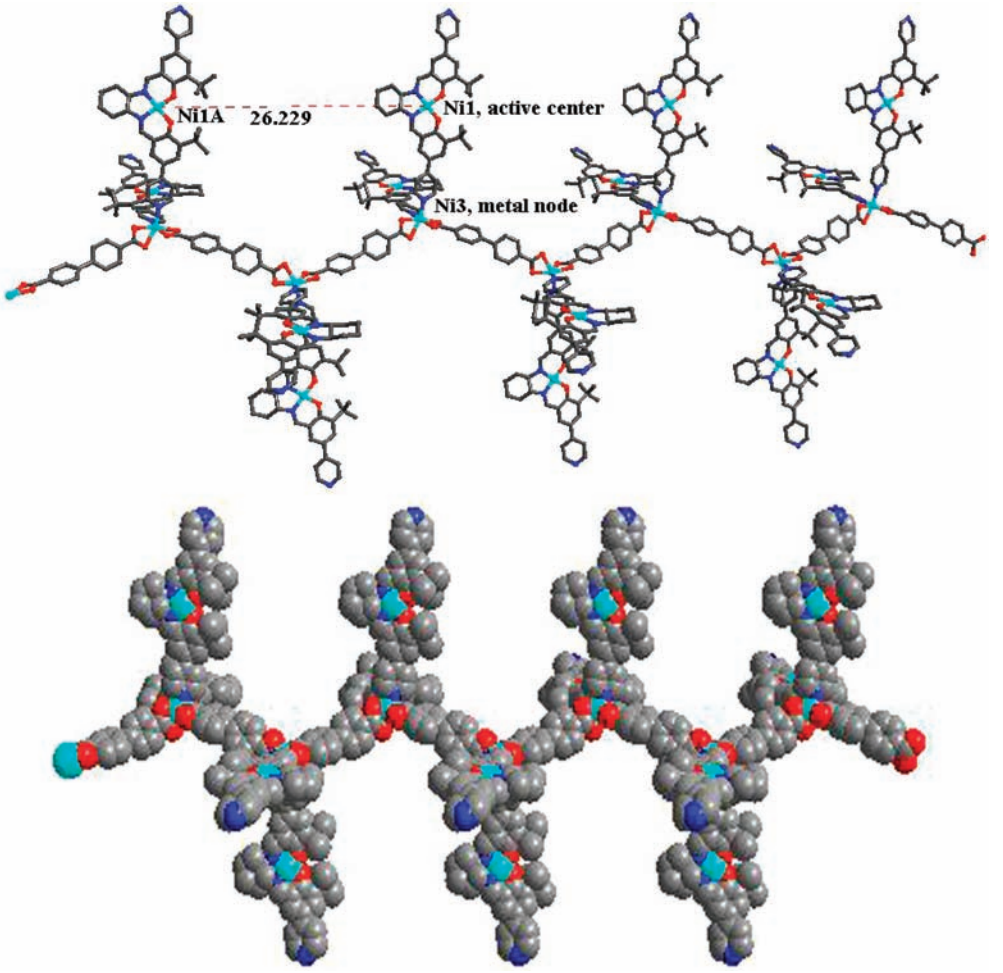

Figure 2. Top, a view of Ball-and-Stick and representation of the 1D chain in **2R**. Bottom, a Space-filling model of the 1D chain in **2R**. Color code: dark-gray, carbon; blue, nitrogen; red, oxygen; blue-green, nickel.

nickel center Ni3 (Ni4), while another one remains uncoordinated, which is similar to those of Zn(salen) polymers[45] and metallomacrocycles,[48,49] and homochiral porous material POST-1 ($[Zn_3O(L)_6]\cdot 2H_3O\cdot 12H_2O)_n$ (L = 4-aminopyridine amide derivative of tartaric acid) being first used as coordination polymer for asymmetric catalysis reaction,[50] but different from the coordination polymer $[Ni_2(oba)_2(bpy)_2(H_2O)_2]\cdot$bpy (**6**) using bpy as cross-linkers.[47b] Changes of the different nickel precursors ($Ni(OAc)_2\cdot 4H_2O$ and $NiCl_2\cdot 6H_2O$) or the stoichiometric ratio of the $Ni(NO_3)_2$, H_2L, and bpdc (3:1:1, 4:1:1) still gave the same product **2R** under the same conditions, confirmed by the powder X-ray diffraction (PXRD) (Supporting Information, Figure S7). The two independent NiN_2O_2 planes have dihedral angles of 24.3° and 25.9° with the coordinated pyridine rings and of 34.2° and 27.5° with the uncoordinated pyridine rings, respectively. The two NiL units coordinated to a same nickel node are nearly perpendicular (with a dihedral angle of 88.3°). The distance of the two types of nickel centers (e.g., Ni1 and Ni3) is 11.798 Å, while the distance of the two unsaturated active nickel centers (e.g., Ni1 and Ni1B (symmetry operation: $-x+1, y, -z+1/2$)) from the NiL metalloligands anchoring on the same nickel node is 15.877 Å. The resultant 1D coordination polymeric chain exhibits a turning angle (defined by three adjacent metal centers) of 126.33° and a repeating period of 26.229 Å (Figure 2).

In general, when using enantiopure chiral molecules as building blocks, the helical compounds are usually chiral, with the right- or left-handed feature. While right- and left-handed helices are formed in equal amounts within a single crystal to produce a meso compound, achiral or racemic molecules are used as building blocks.[52] Surprisingly, it is of particular interest to note that left- and right-handed helix structures based on the enantiopure metalloligands NiL and achiral molecules ($bpdc^{2-}$ and nickel) are observed in both the homochiral coordination polymers **2R** and **2S** (Figure 3, Supporting Information, Figure S3). The chiral molecules NiL (*RR*-NiL) in **2R** coordinated to the nickel node via the terminal nitrogen of the pyridyl groups are almost perpendicular to the helical chains, while the helical backbone are actually constructed from achiral units (nickel and bpdc ligand). Therefore, in this case, the molecular chirality of *RR*-NiL serves as an external chiral source to interact with the helix made of achiral building blocks. The phenomenon is different from the internal induction in which the chirality of the molecular building block forms an inherent part of the helical backbone (e.g., the helicity of DNA based on D-sugars).[52] And also, the chiral sources (cyclohexyl) in **2R** are remote from the helical chains (e.g., C13···Ni3 = 12.9969 Å, C18···Ni3 = 11.7099 Å), which result in almost no chiral induction interaction to the helical backbone chains constructed from achiral building blocks.[52b] So, it is not a surprise that there exist left- and

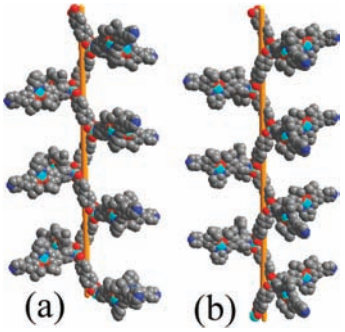

Figure 3. View of left-handed (a) and right-handed (b) helix polymeric chains of **2R**.

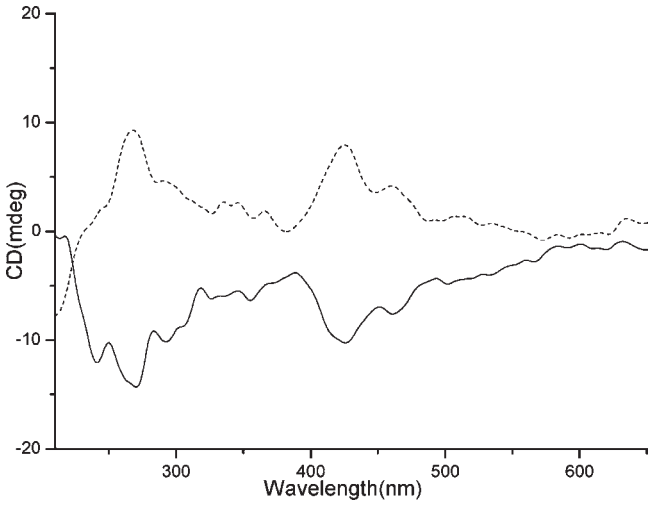

Figure 4. CD spectra of **2R** (solid line) and **2S** (dashed line).

right-handed helices in the homochiral coordination polymers **2R** and **2S**, but the metalloligands NiL coordinated to the backbone of the left- and right-handed helices in **2R** keep the same absolute configuration (Supporting Information, Figure S1 and S2), which is the enantiomer of that in **2S** (Supporting Information, Figure S1 and S3).

Weak interchain $\pi\cdots\pi$ interactions exist between extended π conjugated NiL units and pyridyl groups (plane-to-plane separation ca. 3.90 Å, respectively, Supporting Information, Figure S4). There exist C−H$\cdots\pi$ interactions between the cyclohexyl groups and coordinated pyridyl groups (the distance is ca. 3.59 and 3.49 Å, respectively Supporting Information, Figure S5). The void space between the adjacent polymeric chains is occupied by dimethylformamide (DMF) molecules (Supporting Information, Figure S6). Interestingly, the supermolecular structure (Supporting Information, Figure S6) is further stabilized by the weak hydrogen-bonding interactions (Supporting Information, Figure S5) formed by the DMF molecules with uncoordinated pyridyl groups, as well as the phenol hydroxyl groups with *tert*-butyl groups. TGA (Supporting Information, Figure S9) and PXRD (Supporting Information, Figure S10) measurements indicate that the framework of **2R** remains intact upon complete removal of solvent DMF molecules and remains stable up to about 305 °C.

IR spectra of complexes **1R**, **1S**, **2R**, and **2S** (Supporting Information, Figure S11) show that the C═N stretching vibrations shift to about 1597 cm^{-1} expected for the nickel coordinated salen ligand, H_2L.[9,46] The absence of the expected characteristic band at 1689 cm^{-1} for the protonated carboxylate groups (appears at ca. 1679 cm^{-1}) indicates the complete deprotonation of bpdc ligand and coordination to the nickel center[47] for **2R** and **2S**. The solid state UV−vis spectrum of complex **1R** (Supporting Information, Figure S8) with salen ligand presents high intense bands occurring at λ < 500 nm, because of metal-to-ligand and ligand-to-metal charge transfer and intraligand transitions, while one broad band in the visible region at λ = 500−650 nm is attributed to the nonresolved d-d transitions from the four low-lying d orbitals (d_{xz}, d_{yz}, d_{z^2}, d_{xy}) to the empty orbital.[9,10] The solid state UV−vis spectrum of **2R** (Supporting Information, Figure S8) shows similar features to the free complex **1R**, indicating that no change at the Ni(II) coordination center took place during self-assmebly.

Table 1. Effect of Solvent on the Oxidation of Styrene with NaClO Catalyzed by 2R[a]

entry	solvent (5 mL)	conversion[b](%)	epoxide (%)	selectivity[c] (%)
1	CH_2Cl_2	34	19	56
2	CH_3CN	28	13	46
3	CH_3COCH_3	23	11	48
4	CH_3OH	22	10	45
5	DMF	trace		
6	CH_3CN (60 °C)	36	9	25

[a] Reaction conditions: styrene (0.5 mmol); NaClO (2 mmol); Catalyst (0.01 mmol); T = 25 °C. [b] Based on substrate taken. [c] Epoxide yield/% Conversion.

The cyclic voltammogram (Supporting Information, Figure S12) of complex **1R** shows the anodic peak potential Epa= −1.18 V and the cathodic peak potential Epc= −1.31 V, which are indicative of a quasi-reversible electrode process, corresponding to the Ni^{3+}/Ni^{2+} couple of the NiL.[9,51] The values of Epa and Epc of **2R** are −0.98, −1.11 V, respectively. These peak potentials are more positive than that of complex **1R**. Interestingly, both of the ΔEp values of **1R** and **2R** are about 0.13 V, which indicates that the coordination polymer **2R** shows the salen nickel electrochemistry property, while the metal node Ni3 shows no electrochemistry property.[53]

The chiral coordination polymers **2R** and **2S** containing unsaturated active centers in NiL can be viewed as self-supported heterogeneous catalysts and prompt us to explore their applications in alkene epoxidation. Compounds **2R** and **2S** are stable in air even after the loss of solvent molecules, different from most of 3D MOFs containing large open channels which are mechanically unstable.[43b] Compounds **2R** and **2S** are insoluble in water and common organic solvents such as DMF, DMSO, CH_2Cl_2, and EtOH. The catalytic activity results from the surface catalytic sites, similar to that of the coordination polymers formed by the reaction of [bis(catechol)salen]Mn^{III} with several di- and trivalent metal ions.[33] Therefore, the samples of **2R** were pestled to powder and dried under vacuum to remove the solvent and then were subjected to ultrasonication for 30 min to increase the surface active sites prior to use. The choice of solvent is crucial for the catalytic epoxidation of alkenes (Table 1). Among dichloromethane, acetonitrile, methanol, acetone, and DMF, the weak donor solvent dichloromethane was chosen as reaction medium because the higher yield epoxide was observed for the epoxidation of styrene. Lower catalytic activity in the presence of a stronger coordinating solvent was observed because the axially

coordinated solvent prevents the oxidant OCl^- from formation of catalytically active intermediate nickel(IV)-oxo species and the assessment of substrates to active centers.[9]

The effect of different oxidants on the catalytic activity of **2R** in the oxidation of styrene was studied (Table 2). When NaOCl, *tert*-BuOOH, H_2O_2, and O_2 were used as the oxygen source in dichloromethane for the oxidation of styrene, the economic domestic bleach NaClO as the best oxidant gave higher conversion and selectivity. Although the oxidant *tert*-BuOOH gave the comparative conversion with that of NaOCl, the epoxide selectivity reduced to only 27%. A series of the above controlled experiments shows that each component is essential for an effective catalytic epoxidation. Neither **2R** (entry 6, Table 2) nor NaClO (entry 5, Table 2) alone is able to catalyze styrene epoxidation. The effect of the temperature on the epoxidation of styrene was also evaluated. Although the conversion of the styrene slightly increased to 36% when the reaction temperature increased to 60 °C in CH_3CN, the epoxide product decreased to only 9% (entry 6, Table 1).

For comparison of the effectiveness of different substituent groups on the aromatic rings of the ligands in nickel complexes, we also synthesized (*R*,*R*)-(-)-1,2-cyclohexanediamino-*N*,*N*′-bis(salicylidene)(Ni) (**3**) and (*R*,*R*)-(-)-1,2-cyclohexanediamino-*N*,*N*′-bis(3-*tert*-butyl-salicylidene)(Ni) (**4**) by a similar procedure to that for complex **1R**. The results of the epoxidation of alkenes by complexes **1R**, **2R**, **3**, **4**, **5**, and **6** are provided in Table 3. Introduction of the *tert*-butyl group (bulky steric hindrance and electron-donating group) in the third position of the aldehyde fragment (entry 4, Table 3) could be responsible for the lower reaction conversion compared with that of the unsubstituted salen(Ni) complex **3** (entry 3, Table 3).[10,11] The reason may be that the bulky steric hindrance *tert*-butyl group is unfavorable for alkene to access the active nickel center. However, the moderate epoxide selectivity (for styrene oxidation, benzaldehyde and other products were also obtained) was quite similar to that of the unsubstituted salen nickel complex (entry 3 and 4, Table 3).[8−11] Interestingly, no significant changes about conversion and selectivity were observed when the pyridyl functional group was introduced to the *para* position of OH group, as in complex **1R** (entries 1 and 4, Table 3). The conversion and epoxide selectivity of the styrene oxidation is higher than the cyclohexene reaction catalyzed by both **1R** (entries 1 and 7, Table 3) and **2R** (entries 2 and 8, Table 3), indicating that the electron-rich olefins are more reactive for oxidation than electron poor ones.[8] Interestingly, the conversion and epoxide selectivity of the styrene and cyclohexene oxidation catalyzed by **2R** as self-supported heterogeneous catalyst are close to that of **1R** (entries 1 and 2, Table 3). The reason may be that the self-supported catalyst **2R** contains much more active centers than those of other heterogeneous supported catalysts such as zeolites.[12] And the arranged regular active centers coordinated to the helical chains may therefore enforce a cooperative reaction pathway resulting in enhanced reaction rates and higher selectivities.[54] The unsaturated active nickel center is far away from the coordination polymeric chain (e.g., the distance of Ni1 and Ni3 is 11.798 Å), and only one terminal pyridyl group is coordinated to the metal node which makes the substrate access easily to get the comparative conversion and selectivity of complex **1**.[25−28] While complexes **5** and **6**, in which the coordination model of nickel ion is similar to those of metal nodes (e.g., Ni3) in **2R** and **2S**, showed no activity for styrene epoxidation (entries 5 and 6, Table 3) under the same conditions. The results further prove that the catalytic activity of **2R** comes from the salen(Ni) metalloligands, but not from Ni3 metal node that is positioned in a distorted octahedral six-coordination geometry without space for substrate insertion.

The supernatant of catalysis system of **2R** did not result in further oxidation of the substrate under identical experimental conditions, and no metal species leaching into the organic phases were detected (<1 ppm) by inductively coupled plasma (ICP) spectroscopic analysis, confirming the heterogeneous nature of the present catalytic system.[31b,c] The FTIR spectra (Supporting Information, Figure S11) and PXRD patterns (Supporting Information, Figure S13) of the catalyst **2R** before and after the reaction were compared. The results show that no changes are observed in the FTIR and PXRD before and after reaction,

Table 2. Effect of Various Oxidants on the Oxidation of Styrene Catalyzed by 2R[a]

entry	oxidant (2 mmol)	conversion[b] (%)	epoxide (%)	selectivity[c](%)
1	NaClO	34	19	56
2	H_2O_2	12	trace	
3	*tert*-BuOOH	33	9	27
4	O_2	trace		
5[d]	NaClO	trace		
6[e]		trace		

[a] Reaction conditions: styrene (0.5 mmol); catalyst (0.01 mmol); CH_2Cl_2 (5 mL); T = 25 °C. [b] Based on substrate taken. [c] Epoxide yield/% conversion. [d] No nickel catalyst. [e] No oxidant.

Table 3. Oxidation of Alkenes Catalyzed by Complex 1 and 2R[a]

entry	substrate (0.5 mmol)	catalyst (0.01 mmol)	conversion[b](%)	epoxide (%)	selectivity[c] (%)
1	styrene	**1R**	39	21	54
2	styrene	**2R**	34	19	56
3	styrene	**3**	62	38	61
4	styrene	**4**	40	27	68
5	styrene	**5**	Trace		
6	styrene	**6**	Trace		
7	cyclohexene	**1R**	29	8	27
8	cyclohexene	**2R**	22	7	32
9	styrene	**2R**[d]	29	17	58
10	styrene	**2R**[e]	22	13	56

[a] Reaction conditions: NaClO (2 mmol); Catalyst (0.01 mmol); CH_2Cl_2 (5 mL); T = 25 °C; t = 24 h. [b] Based on substrate taken. [c] Epoxide yield/% conversion. [d] Second reuse. [e] Third reuse.

dx.doi.org/10.1021/ic102181h |*Inorg. Chem.* 2011, 50, 2191–2198

Table 4. Crystallographic Data for Compounds 1S, 2R, and 2S

	1S	2R	2S
empirical formula	$C_{82}H_{98}N_{10}O_6Ni_2$	$C_{93}H_{99}N_9O_9Ni_3$	$C_{93}H_{99}N_9O_9Ni_3$
formula weight	1437.12	1662.94	1662.94
temperature (K)	298(2)	173(2)	298(2)
cryst syst	monoclinic	orthorhombic	orthorhombic
space group	$P2_1$	$P222_1$	$P222_1$
a (Å)	9.789(3)	27.486(4)	27.514(3)
b (Å)	24.528(8)	11.0171(18)	11.0404(15)
c (Å)	16.262(5)	26.229(4)	26.236(4)
β (deg)	106.721(5)	90	90
V (Å^3)	3739(2)	7942(2)	7969.6(18)
Z	2	4	4
D_{calc} (Mg m^{-3})	1.276	1.391	1.386
crystal size (mm)	0.12 × 0.10 × 0.08	0.15 × 0.12 × 0.08	0.15 × 0.12 × 0.08
μ (mm^{-1})	0.563	0.771	0.768
F(000)	1528	3504	3504
θ_{max}, θ_{min} (deg)	27.46, 2.17	27.49, 2.00	27.47, 2.00
index range h	−12→12	−32→35	−35→32
k	−31→30	−14→14	−13→14
l	−15→21	−34→34	−34→34
R_{int}	0.0477	0.0519	0.0519
absolute structure parameter	0.002(1)	0.028(1)	0.055(2)
no.of indep refls	9468	15332	14510
no. of obsd refls	15131	18192	18237
no. of variables	917	1071	1081
final R indices [$I > 2\sigma(I)$]: R_1[a], wR_2[b]	0.0524, 0.0989	0.0592, 0.1686	0.0655, 0.1936
final R indices [all data]: R_1[a], wR_2[b]	0.0890, 0.1164	0.0710, 0.1821	0.0854, 0.2230
GOF on F^2	0.992	1.211	1.043
largest diff.Peak*(hole)(e Å^{-3})	0.239(−0.376)	1.017 (−0. 850)	1.183 (−0. 850)

[a] $R_1 = \Sigma||F_o| - |F_c||/\Sigma|F_o|$, $wR_2 = [\Sigma(|F_o|^2 - |F_c|^2)^2/\Sigma(F_o^2)^2)]^{1/2}$.

which indicate that the self-supported catalyst remains stable, even though in the basic reaction medium. Encouraged by the persistence of catalytic activity for **2R**, we examined its recyclability. Samples of **2R** were easily recovered by centrifugation after catalytic reaction and rinsed by dichloromethane before being used again for styrene epoxidation. Remarkably, after three cycles no loss of epoxide selectivity and only a slight loss of conversion were observed (Table 3). The loss of conversion may be caused by the loss of the catalyst during the recovery process.

CONCLUSIONS

In summary, we have successfully synthesized 1D homochiral nickel coordination polymers based on pyridyl substituted metalloligands salen(Ni) units via two self-assembly methods, in which only one pyridyl group of the NiL unit as unbridging pendant metalolligands coordinated to polymeric chains. It is very interesting that both of the homochiral coordination polymers **2R** and **2S** contain left- and right-handed helical chains made of the achiral building blocks, while the NiL as remote external chiral source is perpendicular to the backbone of the helices. The compounds show catalytic activity comparable to their homogeneous counterpart in alkene epoxidation reaction and exhibit great potential as recyclable catalysts. This assembly approach provides a facile and efficient strategy to synthesize self-supported catalysts.

EXPERIMENTAL SECTION

Materials and Instruments. Ligands (*R*,*R*)-(-)-1,2-cyclohexanediamino-*N*,*N*′-bis(3-*tert*-butyl-5-(4-pyridyl)salicylidene[46] (*RR*-H_2L), (*S*,*S*)-(-)-1,2-cyclohexanediamino-*N*,*N*′-bis(3-*tert*-butyl-5-(4-pyridyl) salicylidene)[46] (*SS*-H_2L) (Supporting Information, Scheme S1) and complexes dibenzoatodipyridinnenickel(II) (**5**), $[Ni_2(oba)_2(bpy)_2(H_2O)_2]\cdot$bpy (**6**) were synthesized according to literature procedures. Unless otherwise stated all other chemicals are commercial available, and used without further purification. Fourier-transform infrared (FT-IR) spectra were taken on a Magna 750 FTIR spectrometer with samples as KBr pellets in the range of 450−4000 cm^{-1}. PXRD patterns were recorded on a Rigaku-Dmax2500 diffractometer using Cu Kα radiation (λ = 0.154 nm). GC-MS measurements were performed on a Varian 450-GC/240-MS. Elemental analyses of C, H, and N were determined using a Vario MICRO E III elemental analyzer. Thermogravimetric analyses were performed on an NETZSCH STA 449C unit at a heating rate of 10 °C/min under nitrogen atmosphere. Solid-state circular dichroism (CD) spectra of compounds **2R** and **2S** were recorded using a JASCO J-810 spectrometer. For each CD measurement about 0.5 mg of crystalline sample was taken to be mixed with 40 mg of dried and well ground KCl powder. This mixture was then pressed into a disk by a literature method.[41] The UV−vis diffuse reflectance spectra were measured on a Perkin Elmer Lambda 900 UV/vis spectrometer equipped with an integrating sphere over the 200−2000 nm wavelength range at room temperature. A $BaSO_4$ plate was used as reference material (100% reflectance). Cyclic voltammogram (CV) was recorded

dx.doi.org/10.1021/ic102181h |*Inorg. Chem.* 2011, 50, 2191–2198

on a 384B polarographic analyzer. An epsilon Electrochemical Workstation connected to a Digital-586 personal computer was used for control of the electrochemical measurements and for data collection. A conventional three-electrode system was used. The working electrode was a modified carbon paste electrode (CPE). An Ag/AgCl (saturated KCl) electrode was used as a reference electrode and Pt gauze as a counter electrode. All potentials were measured and reported versus the Fc^+/Fc couple. The measurements were carried out under N_2, in degassed DMF (distilled from CaH_2 under N_2), using 0.1 M $N(n\text{-}Bu)_4ClO_4$ as the supporting electrolyte. The CPE was fabricated as follows:[55] 25 mg graphite powder and 3 mg compound (**1R** and **2R**) were mixed and ground together by agate mortar and pestle to achieve an even mixture, then 0.10 mL of paraffin oil was added to the above mixture and stirred with a glass rod, then the mixture was used to paste on a 5 mm diameter carbon bar, and the surface was pressed tightly by a clean knife. Electrical contact was established through a carbon bar electrode.

Crystal structure determinations of compounds **1S**, **2R**, and **2S** were collected with a Saturn 70 single-crystal diffractometer equipped with graphite-monochromated Mo Kα radiation (λ = 0.71073 Å). The Crytal-Clear software was used for data reduction and empirical absorption correction.[56a] The structures of compounds **1S**, **2R**, and **2S** were solved by direct methods and successive Fourier difference syntheses, and refined by the fullmatrix least-squares on F^2.[56b] Details of the crystal parameters, data collection, and refinement are summarized in Table 4. Selected bond lengths and bond angles are listed in Supporting Information, Table S1.

Synthesis of Complex *RR*-NiL (1R). Ligand *RR*-H_2L (1 mmol) was dissolved in MeOH (40 mL), and $Ni(OAc)_2 \cdot 4H_2O$ (1 mmol) was added to give to a yellow solution. The reaction mixture was stirred under reflux for 24 h and then concentrated to about 10 mL. The yellow products were filtered and washed with cold MeOH and diethyl ether, collected, and dried under vacuum. Yield: 86%. Anal. Calcd for **1R**, $C_{38}H_{42}N_4O_2Ni$: C, 70.71; H, 6.56; N, 8.68. Found: C, 70.65; H, 6.52; N, 8.62%. IR (KBr, cm^{-1}): 3391 (br), 2942 (m), 2864 (w), 1597 (s), 1552 (m), 1439 (m), 1405 (m), 1346 (m), 1280 (m), 1224 (m), 1173 (m), 1017 (w), 902 (w), 830 (m), 788 (w), 649 (m), 576 (w).

Synthesis of Coordination Polymer 2R. Method A: A mixture of $Ni(NO_3)_2 \cdot 6H_2O$ (0.02 mmol), *RR*-NiL (**1R**) (0.02 mmol), and bpdc (0.02 mmol) was placed in Teflon-lined stainless autoclave containing DMF (10 mL) and EtOH (1 mL). The mixture was heated at 80 °C for 24 h and then cooled to room temperature. The red brown crystals were filtered and washed with DMF, EtOH, and diethyl ether, and collected and dried in air. Yield: 64.2% (based on Ni). Anal. Calcd for **2R**, $C_{93}H_{99}N_9O_9Ni_3$: C, 67.17; H, 6.00; N, 7.58. Found: C, 67.02; H, 5.94; N, 7.49%. IR (KBr, cm^{-1}): 3388 (b), 3069 (w), 3026 (w), 2949 (m), 2865 (w), 1679 (s), 1597 (s), 1551 (m), 1434 (s), 1406 (m), 1385 (m), 1347 (m), 1324 (m), 1281 (m), 1223 (m), 1174 (m), 1087 (m), 1051 (w), 1025 (w), 991 (w), 899 (w), 834 (w), 820 (w), 787 (w), 650 (m), 575 (w). Method B: A mixture of $Ni(NO_3)_2 \cdot 6H_2O$ (0.04 mmol), *RR*-H_2L (0.02 mmol), and bpdc (0.02 mmol) (or the ratio change to 3:1:1; 4:1:1) was placed in Teflon-lined stainless autoclave containing DMF (10 mL) and EtOH (1 mL). The mixture was heated at 80 °C for 24 h and then cooled to room temperature. The red brown crystals were filtered and washed with DMF, EtOH, and diethyl ether, and collected and dried in air. Using $Ni(OAc)_2 \cdot 4H_2O$ or $NiCl_2 \cdot 6H_2O$ in a similar procedure also obtained the same product. The PXRD, elemental analysis, and IR of the obtained product were similar to that of the method A.

Synthesis of Complex (*R,R*)-(-)-1,2-cyclohexanediamino-*N,N′*-bis(salicylidene)(Ni) (3). The synthesis procedure was similar to that of **1R** except using ligand (*R,R*)-(-)-1,2-cyclohexanediamino-*N,N′*-bis(salicylidene).[11] Yield: 87% (based on Ni). Anal. Calcd for **3**, $C_{20}H_{20}N_2O_2Ni$: C, 63.37; H, 5.32; N, 7.39. Found: C, 63.44; H, 5.38; N, 7.43%. IR (KBr, cm^{-1}): 3048 (w), 3026(w), 2932 (m), 2856 (w), 1599 (s), 1537 (m), 1469 (m), 1455 (m), 1393 (w), 1349 (m), 1325 (m), 1224 (w), 1201 (w), 1147 (w), 1124 (w), 1045 (w), 1027 (w), 908 (w), 847 (w), 811 (w), 760 (w), 739 (w), 621 (w).

Synthesis of Complex (*R,R*)-(-)-1,2-cyclohexanediamino-*N,N′*-bis(3-*tert*-butyl-salicylidene)(Ni) (4). The synthesis procedure was similar to that of **1R** except using ligand (*R,R*)-(-)-1,2-cyclohexanediamino-*N,N′*-bis(3-*tert*-butyl-salicylidene).[46] Yield: 84% (based on Ni). Anal. Calcd for **3**, $C_{28}H_{36}N_2O_2Ni$: C, 68.45; H, 7.39; N, 5.70. Found: C, 68.49; H, 7.42; N, 5.67%. IR (KBr, cm^{-1}): 3056 (w), 3007 (w), 2944 (m), 2901 (w), 2865 (w), 1598 (s), 1539 (m), 1466 (m), 1420 (m), 1388 (m), 1339 (m), 1318 (m), 1244 (w), 1194 (w), 1144 (w), 1091 (w), 1045 (w), 871 (w), 808 (w), 744 (m), 665 (w).

Catalysis of Alkene Epoxidation. In a typical experiment, a solution of the oxidant (for NaClO buffered to pH = 11 with a solution of Na_2HPO_4) was stirred at designated temperature in a solution of solvent enriched with substrate, the nickel catalyst (substrate/catalyst =1 :0.025, phase transfer catalyst benzyltributylammoniumchloride was added to the CH_2Cl_2 solution for complexes **1R 3**, **4** and **5**; while for **2R** and **6**, no phase transfer reagent was employed), and internal standard *n*-decane. Aliquots of organic layer were withdrawn at chosen intervals of time and subjected to gas chromatographic analysis for products. After being used for the catalytic reaction, the mixture was centrifuged at 8000 rpm for 3 min. The supernatant solution was decanted for analysis by GC. The remaining solid was washed with dichloromethane before being dried in air for 0.5 h prior to being reused.

■ ASSOCIATED CONTENT

Supporting Information. Procedures for syntheses of 1S and 2S; CIF files, IR spectra, UV−vis spectra, CV, TGA, and PXRD diagrams and supplementary figures. This material is available free of charge via the Internet at http://pubs.acs.org.

■ AUTHOR INFORMATION

Corresponding Author

*Fax: +86 59183796710. Phone: +86 059183796710. E-mail: rcao@fjirsm.ac.cn.

■ ACKNOWLEDGMENT

We acknowledge the financial support from the 973 Program (2011CB932504, 2007CB815303), NSFC (20731005, 20821061, 21003128), CAS and FJIRSM (SZD07002). We also acknowledge Prof. Jian Zhang, Hui Zhang, Xiaoying Huang, and Jiutong Chen for the crystal structures determination.

■ REFERENCES

(1) McGarrigle, E. M.; Gilheany, D. G. *Chem. Rev.* **2006**, *105*, 1563–1602.

(2) Zhang, W.; Loebach, J. L.; Wilson, S. R.; Jacobsen, E. N. *J. Am. Chem. Soc.* **1990**, *112*, 2801.

(3) Irie, R.; Noda, K.; Iro, Y.; Matsumoto, N.; Katsuki, T. *Tetrahedron Lett.* **1990**, *31*, 7345.

(4) Bhattacharjee, S.; Jeong, K.; Jeong, S.; Ahn, W. *New J. Chem.* **2010**, *34*, 156–162.

(5) Mouri, S.; Chen, Z.; Matsunaga, S.; Shibasaki, M. *Chem. Commun.* **2009**, 5138–5140.

(6) Shepherd, N. E.; Tanabe, H.; Xu, Y.; Matsunaga, S.; Shibasaki, M. *J. Am. Chem. Soc.* **2010**, *132*, 3666–3667.

(7) Gupta, K. C.; Sutar, A. K. *Coord. Chem. Rev.* **2008**, *252* 1420–1450.

(8) (a) Yoon, H.; Burrows, C. J. *J. Am. Chem. Soc.* **1988**, *110*, 4087–4089. (b) Mirkhani, V.; Moghadam, M.; Tangestaninejad, S.;

Mohammadpoor-Baltork, I.; Shams, E.; Rasouli, N. *Appl. Catal., A* **2008**, *334*, 106–111.
(9) Chatterjee, D.; Mukherjee, S.; Mitra, A. *J. Mol. Catal. A: Chem.* **2000**, *154*, 5–8.
(10) Ferreira, R.; García, H.; Castro, B. d.; Freire, C. *Eur. J. Inorg. Chem.* **2005**, 4272–4279.
(11) Castro, B. d.; Ferreira, R.; Freire, C.; García, H.; Palomares, E. J.; Sabater, M. J. *New J. Chem.* **2002**, *26*, 405–410.
(12) Wang, Z.; Chen, G.; Ding, K. *Chem. Rev.* **2009**, *109*, 322–359.
(13) Gladysz, J. A. *Chem. Rev.* **2002**, *102*, 3215.
(14) Maurya, M. R.; Titinchi, S. J.J.; Chand, S. *J. Mol. Catal. A: Chem.* **2000**, *201*, 119–130.
(15) Chatterjee, D.; Mitra, A. *J. Mol. Catal. A: Chem.* **1999**, *144*, 363–367.
(16) Ayala, V.; Corma, A.; Iglesias, M.; Rincón, J. A.; Sánchez, F. *J. Catal.* **2004**, *224*, 170–177.
(17) Phan, A.; Doonan, C. J.; Uribe-Romo, F. J.; Knobler, C. B.; O'Keeffe, M.; Yaghi, O. M. *Acc. Chem. Res.* **2010**, *43*, 58–67.
(18) Li, J.; Kuppler, R. J.; Zhou, H. *Chem. Soc. Rev.* **2009**, *38*, 1477–1504.
(19) (a) Guo, Z.; Cao, R.; Wang, X.; Li, H.; Yuan, W.; Wang, G.; Wu, H.; Li, J. *J. Am. Chem. Soc.* **2009**, *131*, 6894–6895. (b) Xie, L.; Lin, J.; Liu, X.; Wang, Y.; Zhang, W.; Zhang, J.; Chen, X. *Inorg. Chem.* **2010**, *49*, 1158–1165. (c) Li, K. H.; Olson, D. H.; Seidel, J.; Emge, T. J.; Gong, H. W.; Zeng, H. P.; Li, J. *J. Am. Chem. Soc.* **2009**, *131*, 10368. (d) Dai, F.; Dou, J.; He, H.; Zhao, X.; Sun, D. *Inorg. Chem.* **2010**, *49*, 4117–4124. (e) Liu, d.; Ren, Z.; Li, H.; Lang, J. P.; Li, N.; Abrahams, B. F. *Angew. Chem., Int. Ed.* **2010**, *49*, 4767–4770.
(20) Spokoyny, A. M.; Kim, D.; Sumrein, A.; Mirkin, C. A. *Chem. Soc. Rev.* **2009**, *38*, 1218–1227.
(21) Düren, T.; Bae, Y.; Snurr, R. Q. *Chem. Soc. Rev.* **2009**, *38*, 1237–1247.
(22) Murray, L. J.; Dincă, M.; Long, J. R. *Chem. Soc. Rev.* **2009**, *38*, 1294–1314.
(23) Uemura, T.; Yanai, N.; Kitagawa, S. *Chem. Soc. Rev.* **2009**, *38*, 1228–1236.
(24) Wang, Z.; Cohen, S. M. *Chem. Soc. Rev.* **2009**, *38*, 1315–1329.
(25) Ma, L.; Abney, C.; Lin, W. *Chem. Soc. Rev.* **2009**, *38*, 1248–1256.
(26) Lee, J.; Farha, O. K.; Roberts, J.; Scheidt, K. A.; Nguyen, S. T.; Hupp, J. T. *Chem. Soc. Rev.* **2009**, *38*, 1450–1459.
(27) Farrusseng, D.; Aguado, S.; Pinel, C. *Angew. Chem., Int. Ed.* **2009**, *48*, 7502–7513.
(28) Corma, A.; García, H.; Xamena, F. X. L. i. *Chem. Rev.* **2010**, *110*, 4606–4655.
(29) Hong, D.; Hwang, Y. K.; Serre, C.; Férey, G.; Chang, J. *Adv. Funct. Mater.* **2009**, *19*, 1537–1552.
(30) Hasegawa, S.; Horike, S.; Matsuda, R.; Furukawa, S.; Mochizuki, K.; Kinoshita, Y.; Kitagawa, S. *J. Am. Chem. Soc.* **2007**, *129*, 2607–2614.
(31) (a) Wu, C.; Lin, W. *Angew. Chem., Int. Ed.* **2007**, *46*, 1075–1078. (b) Hu, A.; Ngo, H. L.; Lin, W. *Angew. Chem., Int. Ed.* **2003**, *42*, 6000–6003. (c) Hu, A.; Ngo, H. L.; Lin, W. *J. Am. Chem. Soc.* **2003**, *125*, 11490–11491.
(32) Cho, S.; Ma, B.; Nguyen, T. S.; Hupp, J. T.; Albrecht-Schmitt, T. E. *Chem. Commun.* **2006**, 2563–2565.
(33) Cho, S.; Gadzikwa, T.; Afshari, M.; Nguyen, T. S.; Hupp, J. T. *Eur. J. Inorg. Chem.* **2007**, 4863–4867.
(34) Jung, S.; Cho, W.; Lee, H. J.; Oh, M. *Angew. Chem., Int. Ed.* **2009**, *48*, 1459–1462.
(35) Jung, S.; Oh, M. *Angew. Chem., Int. Ed.* **2008**, *47*, 2049–2051.
(36) Oh, M.; Mirkin, C. A. *Nature* **2005**, *438*, 651–654.
(37) Heo, J.; Jeon, Y.; Mirkin, C. A. *J. Am. Chem. Soc.* **2007**, *129*, 7712–7713.
(38) Jeon, Y.; Armatas, G. S.; Heo, J.; Kanatzidis, M. G.; Mirkin, C. A. *Adv. Mater.* **2008**, *20*, 2105–2110.
(39) Oh, M.; Mirkin, C. A. *Angew. Chem., Int. Ed.* **2006**, *45*, 5492–5494.
(40) Kitaura, R.; Onoyama, G.; Sakamoto, H.; Matsuda, R.; Noro, S.; Kitagawa, S. *Angew. Chem., Int. Ed.* **2004**, *43*, 2684–2687.
(41) Yuan, G.; Zhu, C.; Xuan, W.; Cui, Y. *Chem.—Eur. J.* **2009**, *15*, 6428–6434.
(42) Bhunia, A.; Roesky, P. W.; Lan, Y.; Kostakis, G. E.; Powell, A. K. *Inorg. Chem.* **2009**, *48*, 10483–10485.
(43) (a) Jeon, Y.; Heo, J.; Mirkin, C. A. *J. Am. Chem. Soc.* **2007**, *129*, 7480–7481. (b) Song, F.; Wang, C.; Falkowski, J. M.; Ma, L.; Lin, W. *J. Am. Chem. Soc.* **2010**, *132*, 15390–15398.
(44) Chen, B.; Zhao, X.; Putkham, A.; Hong, K.; Lobkovsky, E. B.; Hurtado, E. J.; Fletcher, A. J.; Thomas, K. M. *J. Am. Chem. Soc.* **2008**, *130*, 6411–6423.
(45) Li, G.; Zhu, C.; Xi, X.; Cui, Y. *Chem. Commun.* **2009** 2118–2120.
(46) Morris, G. A.; Zhou, H.; Stern, C. L.; Nguyen, S. T. *Inorg. Chem.* **2001**, *40*, 3222–3227.
(47) (a) Catterick, J.; Thornton, P. *J. Chem. Soc., Dalton Trans.* **1975**, 233–238. (b) Wang, X.; Qin, C.; Wang, E.; Li, Y. G.; Su, Z.; Xu, L.; Carlucci, L. *Angew. Chem., Int. Ed.* **2005**, *44*, 5824–5827.
(48) Li, G.; Yu, W.; Ni, J.; Liu, T.; Liu, Y.; Sheng, E.; Cui, Y. *Angew. Chem., Int. Ed.* **2008**, *47*, 1245–1249.
(49) Li, G.; Yu, W.; Cui, Y. *J. Am. Chem. Soc.* **2008**, *130*, 4582–4583.
(50) Seo, J. S.; Whang, D.; Lee, H.; Jun, S. I.; Oh, J.; Jeon, Y. J.; Kim, K. *Nature* **2000**, *404*, 982.
(51) Azevedo, F.; Freire, C.; Castro, B. D. *Polyhedron* **2002**, *21*, 1695–1705.
(52) (a) Zheng, X.; Lu, T. *CrystEngComm* **2010**, *12*, 324–336. (b) Zhang, J.; Bu, X. *Chem. Commun.* **2009**, 206–208. (c) Morris, R. E.; Bu, X. *Nat. Chem.* **2010**, *2*, 353–361.
(53) Yang, L.; Kinoshita, S.; Yamada, T.; Kanda, S.; Kitagawa, H.; Tokunaga, M.; Ishimoto, T.; Ogura, T.; Nagumo, R.; Miyamoto, A.; Koyama, M. *Angew. Chem., Int. Ed.* **2010**, *49*, 5348–5351.
(54) Haak, R. M.; Wezenberg, S. J.; Kleij, A. W. *Chem. Commun.* **2010**, 2713–2723.
(55) Chen, J.; Wei, C.; Zhang, Z.; Huang, Y.; Lan, T.; Li, Z.; Zhang, W. *Inorg. Chim. Acta* **2006**, *359*, 3396–3404.
(56) (a) Sheldrick, G. M. *SADABS*; University of Göttingen: Göttingen, Germany, 1996. (b) Sheldrick, G. M. *SHELXTL97*; University of Göttingen: Göttingen, Germany, 1997.